Article:
Miele, Y, Jones, SJ, Rossi, F et al. (2 more authors) (2022) Collective Behavior of Urease pH Clocks in Nano- and Microvesicles Controlled by Fast Ammonia Transport. Journal of Physical Chemistry Letters, 13 (8). pp. 1979-1984. ISSN 1948-7185

https://doi.org/10.1021/acs.jpclett.2c00069

Collective Behavior of Urease pH Clocks in Nano- and Micro-Vesicles Controlled by Fast Ammonia Transport

Ylenia Miele[1]#, Stephen J. Jones#[2], Federico Rossi[3] Paul A. Beales[2*] Annette F. Taylor[4*],*

1. Department of Chemistry and Biology, University of Salerno, Fisciano (SA), Italy

2. School of Chemistry and Astbury Centre for Structural Molecular Biology, University of Leeds. Leeds LS2 9JT, UK.

3. Department of Earth, Environmental and Physical Sciences, University of Siena, Siena, Italy; federico.rossi2@unisi.it.

4. Chemical and Biological Engineering, University of Sheffield, Sheffield S1 3JD, UK

#Joint first author

***Corresponding authors**

P.A.Beales@leeds.ac.uk; federico.rossi2@unisi.it; A.F.Taylor@sheffield.ac.uk

ABSTRACT: The transmission of chemical signals via the extracellular solution plays a vital role in collective behaviour in cellular biological systems and may be exploited in applications of lipid vesicles such as drug delivery. Here, we investigated chemical communication in synthetic micro- and nano-vesicles containing urease, in a solution of urea and acid. We combined experiments with simulations to demonstrate that the fast transport of ammonia to the external solution governs the pH-time profile and synchronizes the timing of the pH clock reaction in a heterogeneous population of vesicles. This study shows how the rate of production and emission of a small basic product controls pH changes in active vesicles with a distribution of sizes and enzyme amount, which may be useful in bioreactor or healthcare applications.

TOC GRAPHICS

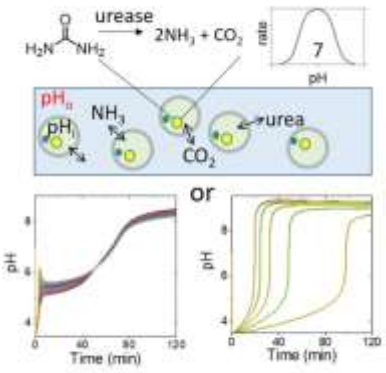

Keywords: vesicles, systems chemistry, collective behavior, non-equilibrium processes, complex systems

Lipid vesicles, or liposomes, are employed in enzyme bioreactors[1, 2] and healthcare applications[3] and also used for the construction of artificial cells with bioinspired dynamics.[4-6] The lipid membranes provide a protective layer with reduced permeability to large molecules and ionic species, and the release of chemicals from the vesicles can be used for molecular communication.[7-9] Here, we investigated the role of the emission of base on the urease reaction with the enzyme confined in synthetic nano- or microvesicles. Urease catalyzes the hydrolysis of urea producing ammonia.[10] In aqueous phase experiments the reaction displays pH-dependent feedback and a rapid switch, referred to as a pH clock, after an induction period where the pH increases slowly.[11] The reaction is widely used in materials and sensing applications[12-17] and urease has been encapsulated in vesicles and polymerosomes,[18-22] however the influence (if any) of compartmentalization and chemical communication on the process is not well understood.

Collective behavior has been mainly investigated with the inorganic Belousov-Zhabotinsky oscillating reaction in emulsion microdroplets or particles and vesicles.[23-26] The period of the reaction depended on catalyst loading and particle size and the products diffused between compartments synchronizing the oscillations or driving more complex responses.[27-31] In the encapsulation of more biologically relevant DNA/RNA transcriptional oscillators[32] and protein oscillators[33], all the reactive species were confined to the microdroplets or vesicles but with urease-encapsulated vesicles, neutral acidic (CO_2) and basic products (NH_3) can diffuse into the surrounding solution. The methods for producing vesicles typically result in a distribution of sizes and enzyme content and so a variation in the pH clock time in individual vesicles might be expected in the absence of a collective response.[34, 35] Theoretical work also suggested that autonomous pH oscillations may occur in urease-vesicles providing there is sufficiently fast transport of acid from the external solution ($P_{H+} > 10^{-5}$ m s^{-1}), but to date these have not been observed in experiments.[36-38] We show that the fast transport of ammonia controls the pH-time

profile and synchronizes the pH change in the vesicles; here the term synchronization is used to refer to a change in behavior (low to high pH) occurring at the same time in a heterogeneous population.

Nanovesicles were prepared using phospholipid film hydration and extrusion and encapsulated a solution of urease, pyranine and HCl (SI 1.2 – 1.3, (Figure 1(a)). As the urease (Sigma-Aldrich type III) is not pure, we report enzyme concentrations in U ml^{-1} rather than μM. The reaction was initiated by addition of urea/HCl solution to vesicle solution in a microcuvette. The ratio of absorbance of pyranine at 450 nm/405 nm was used to estimate the (apparent) pH using a calibration curve with a fitted theoretical relation (SI 1.4, Figure S1)[39, 40] and the total number of vesicles in the 500 μL sample was of the order of $N \sim 10^{11}$ (SI 1.5).

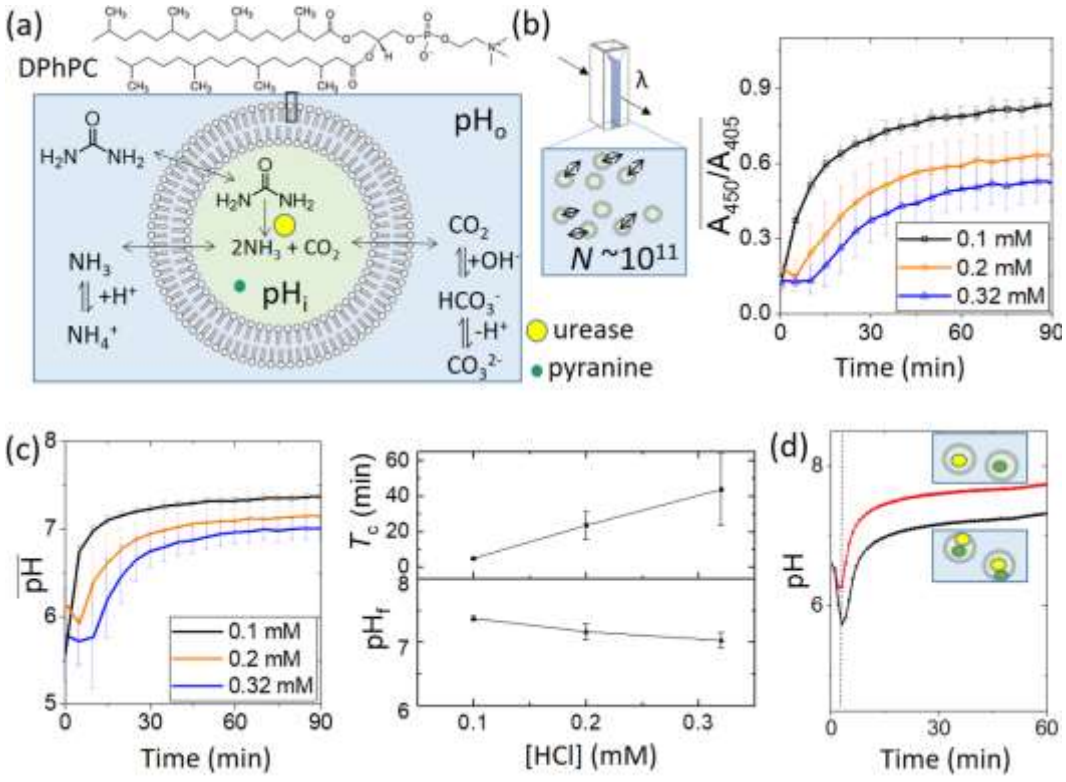

Figure 1. The urease pH clock reaction in nanovesicles of diameter D ~ 200 nm, prepared using 1,2-diphytanoyl-*sn*-glycero-3-phosphocholine (DPhPC), urease (220 U mL^{-1}), HCl (0.1 – 0.32 mM) and pyranine (20 mM), and placed in a solution of urea (50 mM) and HCl (0.1 – 0.32 mM). (a) Schematic of the reaction with urease and pyranine confined to the vesicle (pHi)

and urea in the outer solution (pH_o) and the relevant equilibria. (b) Average ratio of absorbance from vesicles in a microcuvette in a solution of urea/acid and estimated total number of vesicles, *N*, in 500 μL. (c) The average pH in time obtained from the ratio of absorbance in (b); average clock time T_c (here to pH 6.75) and final pH as a function of initial acid concentration. (d) Comparison of pH in time in experiments with [HCl] = 0.2 mM where pyranine is included in the same vesicles as the enzyme (lower black curve), and where pyranine and the enzyme are in separate vesicles (upper red curve). Dotted vertical line corresponds to mixing time. Error bars indicate standard error from three independent experiments.

The ratio, A450/A405, is shown in time, for different initial acid concentrations, in Figure 1(b), and the corresponding pH in Figure 1(c). In the aqueous phase, the clock time, T_c, was defined as the time to reach pH 7, where the urease reaction rate is at a maximum, and it depended on the acid concentration, the urea and the amount of enzyme present in solution.[11] The switch in pH was generally less sharp in the nanovesicles compared to the pH clocks in aqueous phase, with a higher initial pH (after mixing) and lower final pH (SI 1.6). However, the average clock time increased with increasing initial acid concentration as expected (Figure 1(c)).

Evidence for the increase of ammonia in the outer solution was obtained through experiments in which two populations of vesicles were prepared; one with pyranine but no enzyme and one with enzyme and no pyranine. When the two were mixed and urea solution was added, the pH was observed to increase, demonstrating the transfer of ammonia to the urease-free vesicles via the outer solution (Figure 1(d)). To rule out the possibility that enzyme from burst vesicles could contribute to the overall pH change in the cuvette, Triton-X was added to the solution to rupture all the vesicles and no increase in absorbance was observed in time (Figure S3).

The slow increase in pH in the nanovesicles obtained using absorbance measurements may arise from the average of a broad distribution in clock times in a diverse population, or the increase may be slow and synchronized in all vesicles. In order to monitor the pH clock in individual vesicles, the urease reaction was performed in microvesicles prepared by the droplet transfer method (SI 2.1 - 2.2).[19, 41, 42] A sample of vesicles was added to a reaction chamber and the ratio of fluorescence (F458/F405) obtained using confocal microscopy was used to determine the (apparent) pH (SI 2.3 - 2.4). The sizes of the vesicles ranged from 2 – 40 μm (Figure 2(a)) and the total number of vesicles in the chamber was $N \sim 10^4$ (SI 2.5).

A series of confocal images obtained from a typical experiment are shown in Figure 2(b). There was a gradual increase in fluorescence intensity in all vesicles following excitation at 458 nm, corresponding to an increase in pH as the reaction progressed. The coordinated transport of some vesicles was observed after the pH clock, particularly at lower initial acid concentration, possibly arising from convection in the external solution (Figure 2(c)).[43]

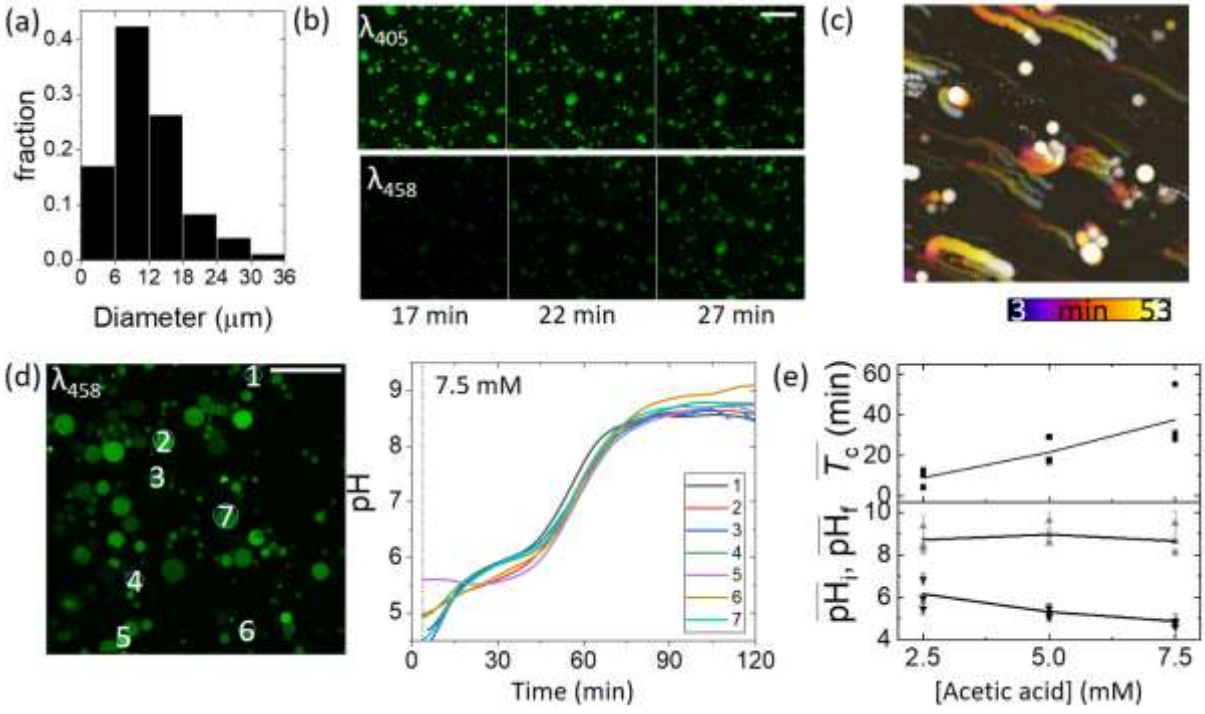

Figure 2. The urease pH clock reaction in synthetic microvesicles, prepared using 1-palmitoyl-

2-oleoyl-*sn*-glycero-3-phosphocholine (POPC), urease (80 U mL^{-1}), pyranine (50 μM) and acetic acid (2.5 -7.5 mM), in a solution of urea (32 mM) and acetic acid (2.5 – 7.5 mM). (a) Fraction of vesicles with a given diameter taken from reaction data with 9 runs. (b). Confocal images in time of the urease pH clock reaction in vesicles with acetic acid 5 mM for two different excitation wavelengths. (c) Image overlay ($\lambda_{458\ nm}$) for the entire time series in an experiment with acid = 2.5 mM showing vesicle motion; coloured bar indicates time. (d) Confocal image of the seven vesicles used in data analysis for 7.5 mM acid and pH in time in each vesicle where dotted vertical line corresponds to mixing time (e) Clock time, T_c and initial (black) and final pH (grey) from experiments with different initial acid concentration. Data points are mean and standard error from seven vesicles in a single experiment and line shows average from the three independent experiments. White scale bar on images = 100 μm.

The pH-time profile in seven individual vesicles is shown in Figure 2(d). The rate of increase of pH in the vesicles was more gradual than in aqueous phase experiments. There was little evidence of a correlation between vesicle diameter and clock time (Figure S6), nor between spatial position of the vesicles and clock time: the timing of the switch from pH 6 to 8 was similar in each vesicle. Overall, there was an increase in clock time and decrease in initial pH with an increase in initial acid concentration as expected (SI 2.6, Figure S7). The average clock time varied between repeats, but the standard deviation was small in each experiment, suggesting the possibility of a synchronized switch in pH in the vesicles mediated by emission of ammonia (Figure 2(e)).

Propagating reaction-diffusion fronts were not observed in either the nano or the microvesicles under these conditions, probably as a result of the low concentration of vesicles. Hence, some insight can be gained from simulations with a simple ODE model of the vesicles and the external solution (SI 3.4). The reaction can be modelled taking into account stochastic effects, however, in other work it was determined that population-level behavior was retained in ODE models.[38, 44] The rate of change of concentration of a species A_i in a vesicle was determined by the reaction and mass transfer rate:[45-47]

$$\frac{dAi}{dt} = f(A_i) + \frac{3P_i}{r}(A_o - A_i) \quad (1)$$

where $f(A_i)$ contains the enzyme reaction and solution equilibria terms (SI 3.1 – 3.2) taken from earlier work,[10, 11, 48] A_o is the concentration of the species in the outer solution, P_i is the permeability coefficient of species i and the radius of the vesicle is r. In the outer solution, the rate of change of concentration of each species, A_o, was given by the reaction rate ($g(A_o)$) and the mass transfer rate (for identical vesicles):

$$\frac{dAo}{dt} = g(A_o) + \phi\frac{3P_i}{r}(A_i - A_o) \quad (2)$$

where $\phi = NV_j/V_o$ = the vesicle volume fraction, which takes into account dilution as a result of the volume change from vesicle to solution. The permeability coefficients for the neutral species were $P_{NH3} = 1 \times 10^{-4}$ m s^{-1}, and $P_{CO2} = 1 \times 10^{-6}$ m s^{-1} and $P_{Urea} = 1 \times 10^{-8}$ m s^{-1} broadly in line with literature values (see SI 3.3).[47, 49] We assumed the permeability of the membrane to all ions (NH_4^+, CO_3^{2-}, HCO_3^-, H^+, OH^-, pyranine) was negligible.

In experiments with nanovesicles of diameter ~ 200 nm, the volume fraction of vesicles was estimated as $\phi = NV_i/V_o \sim 2 \times 10^{-3}$ (see SI 1.6). A similar pH-time profile was obtained in the simulations with the enzyme concentration of [E] = 55 U mL^{-1}, thus assuming an encapsulation efficiency of 25%.[50, 51] Initially, the pH increased rapidly in the vesicles reaching a steady value around pH = 5.5 (Figure 3(a), black curve). The pH switch in the vesicles at 15 minutes was accompanied by an increase in pH the outer solution (Figure 3(a), red curve). The final pH in the vesicles was lower than of the external solution as a result of the buffering effect of pyranine (Figure S8(a)) and the fact that the reaction is not at equilibrium at T = 90 minutes, as less than 2% of the urea was consumed (Figure S8(b)). The model was able to reproduce the experimental trends with changes in initial acid concentration (Figure S9).

The pH-time profile was mainly controlled by the transfer of ammonia to the outer solution (Figure S10). With a lower permeability coefficient of NH_3, the pH increased rapidly in the

vesicle to a high pH with no change in the outer solution whereas for greater P_{NH3} the pH in the vesicle and the external solution were the same (Figure 3(a)). The clock time increased to 90 minutes with $P_{NH3} = 1 \times 10^{-2}$ m s^{-1} and the effect of encapsulation was eliminated: the same result could be obtained by having the enzyme dispersed in the external solution and ammonia diffusing into empty vesicles. This illustrates that compartmentalization played an important role in the pH-time profile in the vesicles – the partial entrapment of ammonia raised the internal pH of the vesicles and enhanced the rate. Nevertheless, the switch was less sharp than in aqueous phase experiments because of the relatively fast loss of ammonia to the outer solution.

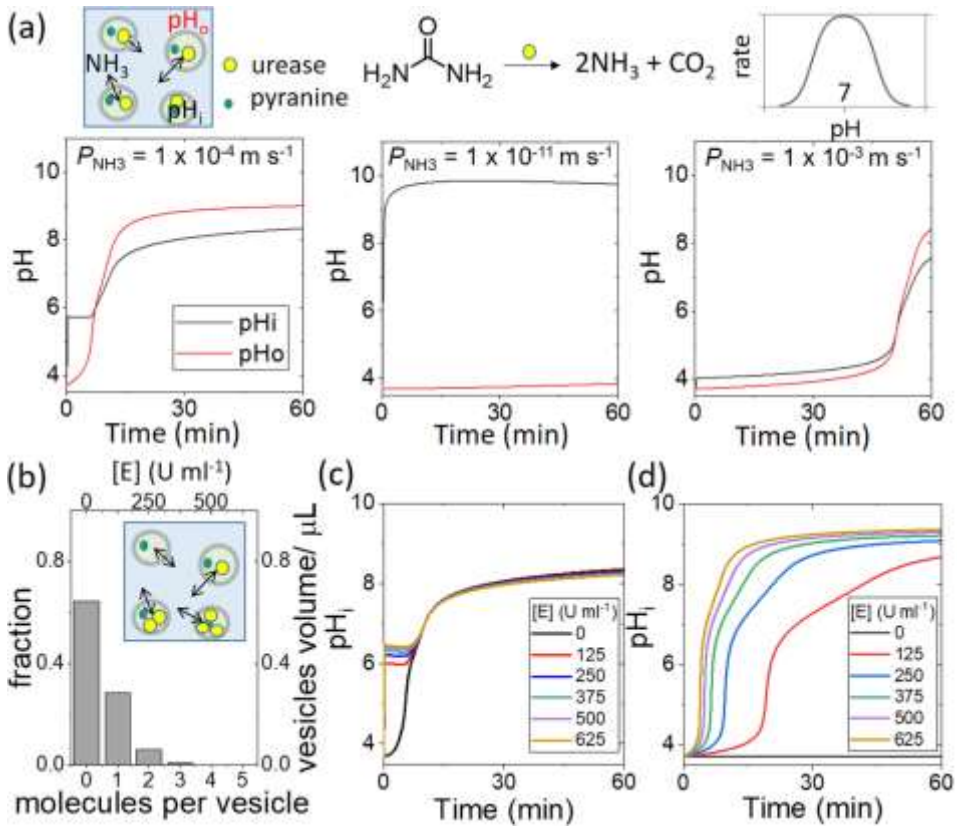

Figure 3. Simulations of the pH clock with a population of nanovesicles, $D = 200$ nm, with [E] = 55 U mL^{-1}, [pyranine] = 5 mM. [HCl] = 0.2 mM, in a solution of [urea] = 50 mM, [HCl] = 0.2 mM and vesicle volume fraction $\phi \sim NV_i/V_o = 2 \times 10^{-3}$. (a) pH in time in identical vesicles (black curve, pH_i) and the outer solution (red curve, pH_o) and effect of the permeability

coefficient of ammonia on the pH clock reaction. (c) Fraction of vesicles with n molecules of urease (Poisson distribution) and equivalent enzyme concentration in U mL^{-1} for a given volume of vesicles (where <E> = 55 U mL^{-1}, including empty vesicles, and total vesicle volume = 1 μL). (d) Synchronized switch in pH for each volume fraction of vesicles given in (c). (e) Range of pH clock times for each volume fraction of vesicles given in (c) with reduced ammonia permeability and enzyme turnover number ($P_{NH3} = 1 \times 10^{-11}$ m s^{-1} and $k_{cat}' = k_{cat}/500$).

Simulations were performed with a distribution of enzyme amount in the vesicles. On average, there was less than one enzyme molecule per vesicle (see SI 3.5.2). The probability of n molecules per vesicle was determined from a Poisson distribution ($P(X=n)$, $\lambda = 0.44$) and the equivalent enzyme concentration in U mL^{-1} was determined from the total number of enzyme molecules in a given volume of the vesicles (Figure 3(b)). The average enzyme concentration for the heterogeneous population (including vesicles with no enzyme) was <E> = 55 U mL^{-1} and the clock time of T_c = 9.6 min was similar to that of the homogenous population with [E] = 55 U mL^{-1} (T_c = 9.3 min). Vesicles with different enzyme loadings in the heterogeneous population have the same clock time, despite the differences in internal pH and enzyme concentration (Figure 3(c)). The potential impact of heterogeneity on the reaction can only be obtained if we reduce both the membrane permeability to ammonia and the enzyme turnover number ($k_{cat}' = k_{cat}/500$ to give the same average clock time of ~ 9 min); then a broad range of clock times is observed (Figure 3(d)).

We also determined the influence of a distribution in enzyme loading and vesicle diameter on the pH clock reaction in the microvesicles. The vesicle volume fraction was $\phi = NV_j/V_o$ = 0.018 and the number of enzyme molecules per vesicle was ~10^5 (SI 2.4). The encapsulation efficiency is generally assumed to be close to 100% using the droplet transfer method, however significant differences in the macromolecular content have been reported.[34, 35] The simulations were undertaken using the experimental probability mass function along with a normal

distribution for the enzyme concentration to obtain a bivariate histogram (SI 3.6) with a range in [E] = 60 – 100 U mL^{-1} and diameter 6 – 36 μm (Figure 4(a)). The membrane permeability to acetic acid (P_{HA}) was also included in these simulations.

The change in pH in the vesicles is shown in Figure 4(b). The profiles are similar to those observed in experiments; there was a rapid increase in the internal pH to ~5.5, then a transition to high pH at around 50 minutes, accompanied by an increase in pH in the surrounding solution arising as a result of the fast transport of ammonia into the outer solution (Figure 4(b)ii). The initial pH was influenced by both the enzyme content and the diameter, with a smaller diameter and smaller enzyme concentration favoring low pH (Figure S11). Again, the synchronized switch in pH does not occur if the permeability coefficient of ammonia/acid and the enzyme turnover number were reduced – in that case, a range of clock times was obtained (Figure 4(c)).

The effect of the concentration of enzyme, [E], on the pH clock with high ammonia permeability was determined in simulations in which the enzyme concentration in each vesicle was identical, but increased from 60 to 100 U ml^{-1} in separate runs. The clock time T_c decreased from 85 to 52 minutes as a result of the increasing total amount of catalyst in the vesicles (Figure 4(c)). In simulations in which the diameter, D, of each vesicle was identical and increased from 6 to 26 μm in separate runs, the clock time increased from 60 to 80 minutes as a result of the reduced rate of transport of ammonia to the external solution (Figure 4(c)). In Figure 4(d), the average clock times are shown for all the simulations with identical [E] or identical D (from Figure 4(c)), compared to the simulation with a distribution in both [E] and D (from Figure 4(b)). The standard deviation in T_c is small for the population with a bivariate distribution as the pH switch is governed by communication between vesicles via the ammonia in the surrounding solution, rather than the internal enzyme concentration or diameter of each vesicle.

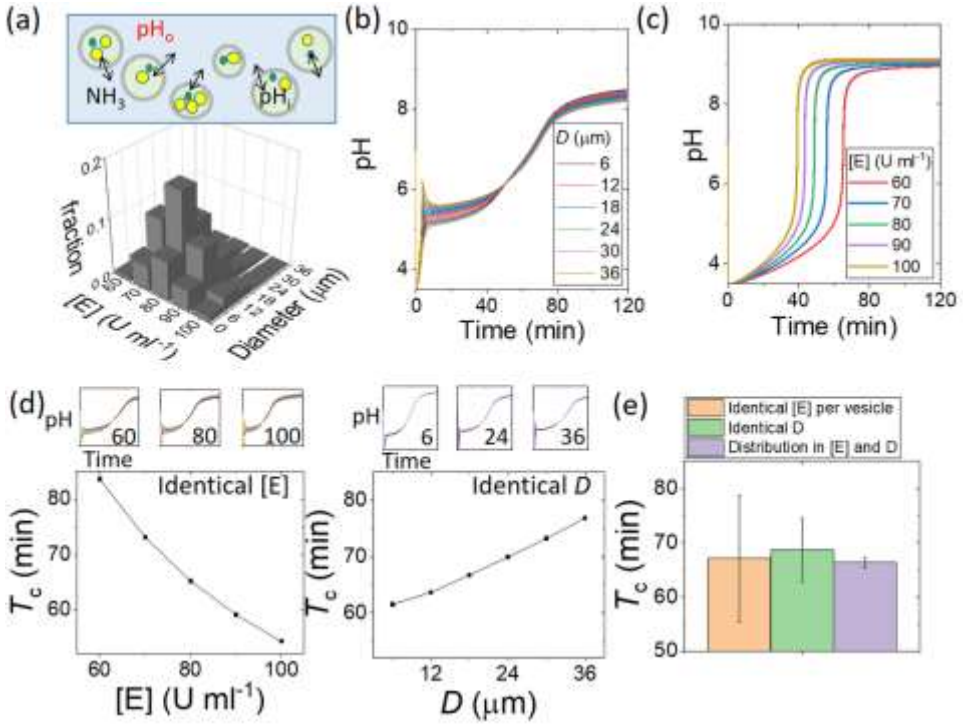

Figure 4. Effect of urease concentration [E] and vesicle diameter, D, on the pH clock in simulations of a population of microvesicles with [pyranine] = 50 μM, in a solution of [urea] = 80 mM and [acetic acid] = 7.5 mM and vesicle volume fraction ϕ = 0.018. (a) Bivariate distribution in the enzyme concentration with <E> = 80 U mL^{-1} and vesicle diameter (D). (b) Synchronized switch in pH in vesicles with the distribution given in (a). (b) Range of pH clock times in vesicles with the distribution given in (a) and with reduced acid/base permeability and enzyme turnover number ($P_{NH3} = P_{HA} = 1 \times 10^{-11}$ m s^{-1} and $k_{cat}' = k_{cat}/50$). (c) Effect of [E] or D on clock time T_c in simulations with a population of vesicles with identical [E] per vesicle and the distribution in D given in (a) or identical D and the distribution in [E] given in (a). (d) Comparison of average and standard deviation (error bars) in clock time in simulations in a population of vesicles with identical [E] or D and a distribution in both [E] and D.

In conclusion, we have shown that the pH-time profile and synchronization of the pH clock in heterogeneous vesicles was controlled by the relatively fast transport and increase of ammonia in the external solution. The behavior was observed in nano- and micro-vesicles with

different phospholipids and acids, thus demonstrating the universal nature of the response. In natural systems, microorganisms such as bacteria or yeast use extracellular signaling to overcome population diversity and change behavior.[52, 53] Ammonia is important in cell-cell communication and the multicellular structures that form in yeast and bacterial colonies. It has been implicated in complex functionality such as metabolic oscillations and colony survival.[54] Further control of the membrane permeability would provide a useful platform for the investigation of more complex collective behavior in populations of synthetic vesicles driven by acid/base changes.[55]

Acknowledgements

YM, FR and AFT acknowledge the support through the COST Action CM1304 (Emergence and Evolution of Complex Chemical Systems). SJ received an EPSRC studentship and PB was supported by EPSRC grant EP/M027929/1.

Supporting information

The following files are available free of charge: supplementary information (.pdf) including the model files in the appendices.

References

(1) Küchler, A.; Yoshimoto, M.; Luginbühl, S.; Mavelli, F.; Walde, P. Enzymatic reactions in confined environments. *Nature Nanotechnology* **2016**, *11,* pp 409-420.

(2) Maiti, S.; Fortunati, I.; Ferrante, C.; Scrimin, P.; Prins, L. J. Dissipative self-assembly of vesicular nanoreactors. *Nature Chemistry* **2016**, *8,* pp 725-731.

(3) Samad, A.; Sultana, Y.; Aqil, M. Liposomal drug delivery systems: An update review. *Curr. Drug Del.* **2007**, *4,* pp 297-305.

(4) Tang, T. Y. D.; Cecchi, D.; Fracasso, G.; Accardi, D.; Coutable-Pennarun, A.; Mansy, S. S.; Perriman, A. W.; Anderson, J. L. R.; Mann, S. Gene-Mediated Chemical Communication in Synthetic Protocell Communities. *ACS Synthetic Biology* **2018**, *7,* pp 339-346.

(5) Trantidou, T.; Friddin, M.; Elani, Y.; Brooks, N. J.; Law, R. V.; Seddon, J. M.; Ces, O. Engineering Compartmentalized Biomimetic Micro- and Nanocontainers. *ACS Nano* **2017**, *11,* pp 6549-6565.

(6) Rideau, E.; Dimova, R.; Schwille, P.; Wurm, F. R.; Landfester, K. Liposomes and polymersomes: a comparative review towards cell mimicking. *Chem. Soc. Rev.* **2018**, *47,* pp 8572-8610.

(7) Soldner, C. A.; Socher, E.; Jamali, V.; Wicke, W.; Ahmadzadeh, A.; Breitinger, H. G.; Burkovski, A.; Castiglione, K.; Schober, R.; Sticht, H. A Survey of Biological Building Blocks for Synthetic Molecular Communication Systems. *IEEE Communications Surveys and Tutorials* **2020**, *22,* pp 2765-2800.

(8) Rampioni, G.; Leoni, L.; Stano, P. Molecular Communications in the Context of 'Synthetic Cells' Research. *IEEE Trans. NanoBiosci.* **2019**, *18,* pp 43-50.

(9) Tomasi, R.; Noël, J. M.; Zenati, A.; Ristori, S.; Rossi, F.; Cabuil, V.; Kanoufi, F.; Abou-Hassan, A. Chemical communication between liposomes encapsulating a chemical oscillatory reaction. *Chemical Science* **2014**, *5,* pp 1854-1859.

(10) Krajewska, B. Ureases I. Functional, catalytic and kinetic properties: A review. *J. Mol. Catal. B: Enzym.* **2009**, *59,* pp 9-21.

(11) Hu, G.; Pojman, J. A.; Scott, S. K.; Wrobel, M. M.; Taylor, A. F. Base-catalyzed feedback in the urea-urease reaction. *J. Phys. Chem. B* **2010**, *114,* pp 14059-14063.

(12) Jaggers, R. W.; Bon, S. A. F. Independent responsive behaviour and communication in hydrogel objects. *Materials Horizons* **2017**, *4,* pp 402-407.

(13) Panja, S.; Boháčová, K.; Dietrich, B.; Adams, D. J. Programming properties of transient hydrogels by an enzymatic reaction. *Nanoscale* **2020**, *12,* pp 12840-12848.

(14) Gao, N.; Li, M.; Tian, L.; Patil, A. J.; Pavan Kumar, B. V. V. S.; Mann, S. Chemical-mediated translocation in protocell-based microactuators. *Nature Chemistry* **2021**, *13,* pp 868-879.

(15) Lvov, Y.; Antipov, A. A.; Mamedov, A.; Möhwald, H.; Sukhorukov, G. B. Urease Encapsulation in Nanoorganized Microshells. *Nano Lett.* **2001**, *1,* pp 125-128.

(16) Muzika, F.; Růžička, M.; Schreiberová, L.; Schreiber, I. Oscillations of pH in the urea-urease system in a membrane reactor. *Phys. Chem. Chem. Phys.* **2019**, *21,* pp 8619-8622.

(17) Maity, I.; Sharma, C.; Lossada, F.; Walther, A. Feedback and Communication in Active Hydrogel Spheres with pH Fronts: Facile Approaches to Grow Soft Hydrogel Structures. *Angewandte Chemie - International Edition* **2021**, *60,* pp 22537-22546.

(18) Madeira, V. M. C. Incorporation of urease into liposomes. *BBA - General Subjects* **1977**, *499,* pp 202-211.

(19) Miele, Y.; Bánsági, T., Jr.; Taylor, A. F.; Stano, P.; Rossi, F. Engineering enzyme-driven dynamic behaviour in lipid vesicles. In *Communications in Computer and Information Science*, 2016; Vol. 587, pp 197-208.

(20) Che, H.; Cao, S.; Van Hest, J. C. M. Feedback-Induced temporal control of "breathing" polymersomes to create self-adaptive nanoreactors. *J. Am. Chem. Soc.* **2018**, *140,* pp 5356-5359.

(21) Wang, X.; Moreno, S.; Boye, S.; Wen, P.; Zhang, K.; Formanek, P.; Lederer, A.; Voit, B.; Appelhans, D. Feedback-Induced and Oscillating pH Regulation of a Binary Enzyme-Polymersomes System. *Chem. Mater.* **2021**, *33,* pp 6692-6700.

(22) Miele, Y.; Medveczky, Z.; Holló, G.; Tegze, B.; Derényi, I.; Hórvölgyi, Z.; Altamura, E.; Lagzi, I.; Rossi, F. Self-division of giant vesicles driven by an internal enzymatic reaction. *Chemical Science* **2020**, *11,* pp 3228-3235.

(23) Toiya, M.; Vanag, V. K.; Epstein, I. R. Diffusively coupled chemical oscillators in a microfluidic assembly. *Angew. Chem. Int. Ed. Engl.* **2008**, *47,* pp 7753-7755.

(24) Tinsley, M. R.; Taylor, A. F.; Huang, Z.; Showalter, K. Emergence of collective behavior in groups of excitable catalyst-loaded particles: Spatiotemporal dynamical quorum sensing. *Phys. Rev. Lett.* **2009**, *102,* p 158301.

(25) Guzowski, J.; Gizynski, K.; Gorecki, J.; Garstecki, P. Microfluidic platform for reproducible self-assembly of chemically communicating droplet networks with predesigned number and type of the communicating compartments. *Lab on a Chip* **2016**, *16,* pp 764-772.

(26) Gentili, P. L.; Giubila, M. S.; Germani, R.; Romani, A.; Nicoziani, A.; Spalletti, A.; Heron, B. M. Optical Communication among Oscillatory Reactions and Photo-Excitable Systems: UV and Visible Radiation Can Synchronize Artificial Neuron Models. *Angew. Chem. Int. Ed. Engl.* **2017**, *56,* pp 7535-7540.

(27) Totz, J. F.; Rode, J.; Tinsley, M. R.; Showalter, K.; Engel, H. Spiral wave chimera states in large populations of coupled chemical oscillators. *Nature Physics* **2018**, *14,* pp 282-285.

(28) Budroni, M. A.; Torbensen, K.; Ristori, S.; Abou-Hassan, A.; Rossi, F. Membrane Structure Drives Synchronization Patterns in Arrays of Diffusively Coupled Self-Oscillating Droplets. *J. Phys. Chem. Letts.* **2020**, *11,* pp 2014-2020.

(29) Yoshikawa, K.; Aihara, R.; Agladze, K. Size-dependent Belousov-Zhabotinsky oscillation in small beads. *J. Phys. Chem. A* **1998**, *102,* pp 7649-7652.

(30) Lawson, H. S.; Holló, G.; Horvath, R.; Kitahata, H.; Lagzi, I. Chemical Resonance, Beats, and Frequency Locking in Forced Chemical Oscillatory Systems. *J. Phys. Chem. Letts.* **2020**, *11,* pp 3014-3019.

(31) Gorecki, J.; Gizynski, K.; Guzowski, J.; Gorecka, J. N.; Garstecki, P.; Gruenert, G.; Dittrich, P. Chemical computing with reaction-diffusion processes. *Philos Trans A Math Phys Eng Sci* **2015**, *373*.

(32) Weitz, M.; Kim, J.; Kapsner, K.; Winfree, E.; Franco, E.; Simmel, F. C. Diversity in the dynamical behaviour of a compartmentalized programmable biochemical oscillator. *Nature Chemistry* **2014**, *6,* pp 295-302.

(33) Litschel, T.; Ramm, B.; Maas, R.; Heymann, M.; Schwille, P. Beating Vesicles: Encapsulated Protein Oscillations Cause Dynamic Membrane Deformations. *Angewandte Chemie - International Edition* **2018**, *57,* pp 16286-16290.

(34) Stano, P.; De Souza, T. P.; Carrara, P.; Altamura, E.; D'Aguanno, E.; Caputo, M.; Luisi, P. L.; Mavelli, F. Recent Biophysical Issues about the Preparation of Solute-Filled Lipid Vesicles. *Mechanics of Advanced Materials and Structures* **2015**, *22,* pp 748-759.

(35) Saito, H.; Kato, Y.; Le Berre, M.; Yamada, A.; Inoue, T.; Yosikawa, K.; Baigl, D. Time-resolved tracking of a minimum gene expression system reconstituted in giant liposomes. *ChemBioChem* **2009**, *10,* pp 1640-1643.

(36) Bánsági, T.; Taylor, A. F. Role of differential transport in an oscillatory enzyme reaction. *J. Phys. Chem. B* **2014**, *118,* pp 6092-6097.

(37) Miele, Y.; Bánsági, T., Jr.; Taylor, A. F.; Rossi, F. Modelling Approach to Enzymatic pH Oscillators in Giant Lipid Vesicles. In *Lecture Notes in Bioengineering*, 2018; pp 63-74.

(38) Straube, A. V.; Winkelmann, S.; Schütte, C.; Höfling, F. Stochastic pH Oscillations in a Model of the Urea-Urease Reaction Confined to Lipid Vesicles. *J. Phys. Chem. Letts.* **2021**, *12,* pp 9888-9893.

(39) Kano, K.; Fendler, J. H. Pyranine as a sensitive pH probe for liposome interiors and surfaces. pH gradients across phospholipid vesicles. *BBA - Biomembranes* **1978**, *509,* pp 289-299.

(40) Clement, N. R.; Gould, J. M. Pyranine (8-Hydroxy-1,3,6-pyrenetrisulfonate) as a Probe of Internal Aqueous Hydrogen Ion Concentration in Phospholipid Vesicles. *Biochemistry* **1981**, *20,* pp 1534-1538.

(41) Pautot, S.; Frisken, B. J.; Weitz, D. A. Production of unilamellar vesicles using an inverted emulsion. *Langmuir* **2003**, *19,* pp 2870-2879.

(42) Walde, P.; Cosentino, K.; Engel, H.; Stano, P. Giant Vesicles: Preparations and Applications. *ChemBioChem* **2010**, *11,* pp 848-865.

(43) Markovic, V. M.; Bánsági, T., Jr.; McKenzie, D.; Mai, A.; Pojman, J. A.; Taylor, A. F. Influence of reaction-induced convection on quorum sensing in enzyme-loaded agarose beads. *Chaos* **2019**, *29*.

(44) Singh, A.; Marcoline, F. V.; Veshaguri, S.; Kao, A. W.; Bruchez, M.; Mindell, J. A.; Stamou, D.; Grabe, M. Protons in small spaces: Discrete simulations of vesicle acidification. *PLoS Comp. Biol.* **2019**, *15*.

(45) Gabba, M.; Poolman, B. Physiochemical Modeling of Vesicle Dynamics upon Osmotic Upshift. *Biophys. J.* **2020**, *118,* pp 435-447.

(46) Missner, A.; Pohl, P. 110 years of the Meyer-Overton rule: Predicting membrane permeability of gases and other small compounds. *ChemPhysChem* **2009**, *10,* pp 1405-1414.

(47) Paula, S.; Volkov, A. G.; Van Hoek, A. N.; Haines, T. H.; Deamer, D. W. Permeation of protons, potassium ions, and small polar molecules through phospholipid bilayers as a function of membrane thickness. *Biophys. J.* **1996**, *70,* pp 339-348.

(48) Krajewska, B.; Ciurli, S. Jack bean (Canavalia ensiformis) urease. Probing acid–base groups of the active site by pH variation. *Plant Physiol. Biochem.* **2005**, *43,* pp 651-658.

(49) Lande, M. B.; Donovan, J. M.; Zeidel, M. L. The relationship between membrane fluidity and permeabilities to water, solutes, ammonia, and protons. *J. Gen. Physiol.* **1995**, *106,* pp 67-84.

(50) Lohse, B.; Bolinger, P. Y.; Stamou, D. Encapsulation efficiency measured on single small unilamellar vesicles. *J. Am. Chem. Soc.* **2008**, *130,* pp 14372-14373.

(51) Colletier, J.-P.; Chaize, B.; Winterhalter, M.; Fournier, D. Protein encapsulation in liposomes: efficiency depends on interactions between protein and phospholipid bilayer. *BMC Biotechnol.* **2002**, *2,* p 9.

(52) Waters, C. M.; Bassler, B. L. Quorum sensing: Cell-to-cell communication in bacteria. In *Annu. Rev. Cell Dev. Biol.*, 2005; Vol. 21, pp 319-346.

(53) De Monte, S.; d'Ovidio, F.; Dano, S.; Sorensen, P. G. Dynamical quorum sensing: Population density encoded in cellular dynamics. *Proc Natl Acad Sci U S A* **2007**, *104,* pp 18377-18381.

(54) Palkova, Z.; Janderova, B.; Gabriel, J.; Zikanova, B.; Pospisek, M.; Forstova, J. Ammonia mediates communication between yeast colonies. *Nature* **1997**, *390,* pp 532-536.

(55) Miller, A. J.; Pearce, A. K.; Foster, J. C.; O'Reilly, R. K. Probing and Tuning the Permeability of Polymersomes. *ACS Central Science* **2021**, *7,* pp 30-38.